

## Numerical Simulation Study on Erosive Wear of ESP

Yanxin Liu<sup>a,b\*</sup>, Runtao Wang<sup>a</sup>, Mingwei Chao<sup>c</sup>, Lijun Zhang<sup>a</sup>

<sup>a</sup> College of Mechanical Engineering, China University of Petroleum, Qingdao 266580, P.R. China

<sup>b</sup> College of Petroleum Engineering, China University of Petroleum, Qingdao 266580, P. R. China

<sup>c</sup> East China Institute of China Petroleum Engineering and Construction Corp, Qingdao 266071, P. R. China

liuyanxin1985@163.com

Wear of electric submersible pump (ESP) in oilfield was caused by high sand content in the high water-cut stage. RNG k- $\epsilon$  turbulence model and discrete phase model are deployed for numerical simulation to study the effect of conditions and structural parameters on the wear of ESP impellers. It is showed that concave side of impeller blades and central area of guide impeller's inner wall are the most eroded area. Wear rate will increase with the rising of sand concentration rate and pump speed. With the rising of particle size, impeller's wear rate will increase first then decrease. The average wear rate of impeller will decrease with the increase of inlet angle, while the rise of outlet angle will make it rise and fall. Results of numerical simulation can be applied to designs of ESPs.

### 1. Introduction

With the continuity of development, a lot of oilfields in china entered the high water-cut stage. Electric submersible pump (ESP) became the major lifting method for increasing and stabilizing oil production in this stage, due to its wide range of displacement and lift, larger power, high adaptability, long inspection period, convenient in management and remarkable economic benefit. However, in the high water-cut stage, ESP's useful life and economic benefit was reduced by the situation of high water-cut, high sand content, high salinity and complication of shaft's condition. Due to the high sand content, severe erosive wear took place on impeller, causing efficiency decrease and affecting the normal operation. In severe cases, perforation took place and leads to pump shell rupture or unit falling. In order to take appropriate protective measures, it is necessary to analyse the wear on the impeller and study the wear mechanism.

According to statistics, in 2014, there were 261 times of pump operation, 59 times of cylinder perforation (Figure 1a) and 2 times of unit falling (Figure 1b) in Shengtuo oilfield. Wear usually took place at seal ring that connects the outlet of impeller and guide impeller, showing a layered circumferential distribution at the inner surface of pump shell, while the perforations start from the inside, holes from outside is smaller than inside. Perforations in pump shell are corresponding to the site of guide impeller, perforations start from the inside, which means perforation in pump shell is caused by the guide impeller's perforation.



(a) Fracture caused by perforations



(b) perforations

Figure 1: The pump barrel perforation failure caused by perforations

Electric submersible centrifugal pump is a kind of centrifugal pump, the present study focused on the slurry pumps and other centrifugal pumps with large diameter, horizontal type, impeller-spiral inlet, high sand content (more than 1%), and large solid particles. Limited research about flow field and erosive wear have been done on ESPs with small diameter, low sand content (less than 0.05%), high pump speed and small particle size. Erosive wear of centrifugal slurry pumps is primarily governed by the particulate motion and concentration (Pagalthivarthi et al, 2007; Pagalthivarthi et al, 2011). Using coating method that head of the impeller was

found to be the most eroded area, and bigger outlet angle will lead to a rise in wear rate. Erosive wear affected by particle size and flow rate was studied. Solids content of the working fluid, the regions of high wall shear, and particle impingement with the walls were major mechanisms associated with the erosive wear (Lee et al, 2002). The failure analysis on the centrifugal slurry pump was performed along with the countermeasures (Khalid et al, 2007). Erosive wear of slurry pumps was observed while accurate location of maximum wear was predicted through CFD (Roudnev et al, 2009). Numerical calculation and analysis on the erosive wear of ESP has been done using discrete phase model (Chen et al, 2015; Wang et al, 2014). They found that the impact wear will be more severe with the increasing in sand particle size and impeller speed. 0.07mm is the critical diameter of the erosion's intensifying.

## 2. Solid and liquid governing equation based on discrete phase model (DPM)

### 2.1 Liquid phase flow governing equation

The type line of impeller and guide impeller blade is curved, as well as the flow line of fluid. Turbulence shows anisotropy. Comparing with the standard  $k-\varepsilon$  turbulence model, RNG  $k-\varepsilon$  turbulence model is more capable of being used due to its modification of turbulence viscosity and consideration on rotation of average flow and swirling flows.

$$\frac{\partial(\rho_f k)}{\partial t} + \frac{\partial(\rho_f u_i k)}{\partial x_i} = \frac{\partial}{\partial x_j} \left( \alpha_k \mu_e \frac{\partial k}{\partial x_j} \right) + G_k + G_p - \rho_f \varepsilon \quad (1)$$

$$\frac{\partial(\rho_f \varepsilon)}{\partial t} + \frac{\partial(\rho_f u_i \varepsilon)}{\partial x_i} = \frac{\partial}{\partial x_j} \left( \alpha_\varepsilon \mu_e \frac{\partial \varepsilon}{\partial x_j} \right) + \frac{\varepsilon}{k} (C_{1\varepsilon} G_k - C_{2\varepsilon} \rho_f \varepsilon) \quad (2)$$

In Eq. (1, 2),  $\rho_f$  is density of fluid,  $k$  is turbulent kinetic energy,  $\varepsilon$  is turbulent energy dissipation rate,  $\mu_e$  is effective viscosity coefficient,  $G_p$  is the turbulent kinetic energy generated by buoyancy,  $G_k$  is the turbulent kinetic energy by velocity gradient.  $C_{1\varepsilon}^*$ ,  $C_{2\varepsilon}$  are the parameters,  $\alpha_k = \alpha_\varepsilon = 1.39$ .

### 2.2 Discrete phase(sand) governing equation

In discrete phase model, the trajectory of particles can be obtained by solving differential equation of particle force in Lagrange coordinate system. Solid particles are subjected to various kinds of forces, such as gravity, all kinds of additional forces, centrifugal force, Coriolis force, Basset force, Magnus force, etc. Governing equation is as follows.

$$m_s \frac{du_s}{dt} = \frac{\pi d_s^3 \rho_s}{6} \left[ \frac{g(\rho_s - \rho_f)}{\rho_s} + F_D + F_V + F_P + F_S + F_{other} \right] \quad (3)$$

In Eq. (3),  $\rho_s$  is density of sand particle,  $g$  is gravity,  $F_D$  is circle resistance of fluid,  $F_V$  is additional mass force,  $F_P$  is additional force by pressure gradient,  $F_{other}$  is sum of centrifugal force, Coriolis force, Basset force, and Magnus Force.

### 2.3 Calculation model on wear rate

Wear rate is defined as the material that worn away by particle force from the surface in unit area.

$$R_{wear} = \sum_{p=1}^N \frac{m_p' C(d_p) f(\alpha) V^{b(V)}}{A_f} \quad (4)$$

In Eq. (4),  $R_{wear}$  is wear rate,  $\text{kg} \cdot \text{m}^{-2} \cdot \text{s}^{-1}$ .  $m_p'$  is mass flow rate presented by sand particle,  $C(d_p)$  is function related to particle size.  $\alpha$  is impact angle between sand particle and wall.  $f(\alpha)$  is function related to the impact angle.  $V$  is impact velocity.  $b(V)$  is function related to the impact velocity.  $A_f$  is the area of calculation unit.  $N$  is granular number that impacts the unit area  $A_f$ .

## 3. Numerical simulation and analysis on wear of ESP

### 3.1 Numerical simulation model on wear of ESP

ESP model W150 with cylindrical impeller is selected. There are 8 blades in impeller while 12 in guide impeller. Single-stage flow channel from impeller inlet to the guide impeller outlet are selected as the calculation area of simulation. Fig.2 is 3D flow field model of single stage ESP.

(1) Model selection and coordinate system setup

DPM and RNG  $k-\varepsilon$  in turbulence model are selected. The displacement is  $150\text{m}^3/\text{d}$ , particle diameter is 0.05mm, sand inlet volume fraction 0.03%, sand density is  $2700\text{kg}/\text{m}^3$ .

For flow channel model, part of the impeller's flow channel is rotating at high speed, while the flow channel between guide impeller and impeller is stationary. For movable flow region, multi reference frame model (MRF), which transforms unsteady flow to steady flow and calculate only the instantaneous flow field in certain impeller position, is selected. The result is in that position only. Set the flow region of impeller in kinetic coordinate system, and rotation speed at 2300r/min



Figure 2: 3D flow field model of single stage ESP

(2) Boundary conditions of inlet and outlet

Liquid phase: selecting velocity-inlet at inlet, outflow at outlet.

Particle phase: escape at outlet

Solid phase inlet: surface injection, particle size, mass flux rate, inert particle, 2700kg/m<sup>3</sup>.

(3) Wall condition

Liquid phase: no slip.

Solid phase: reflect wall.

3.2 Wear analysis of submersible pump based on DPM

(1) Impeller

Figure 3 is the wear distribution of the impeller cover plate. It can be seen from Figure 3 that except for the severe wear at outlet and inlet, rest of the area share an even distribution of wear from the front side, wear rate of places near suction surface is a little bit higher than other places. The front side of back cover suffers the most of wear while the back side takes less damage. The average wear rate of front side is  $5.98 \times 10^{-5} \text{ kg} \cdot \text{m}^{-2} \cdot \text{s}^{-1}$  while it is  $1.11 \times 10^{-4} \text{ kg} \cdot \text{m}^{-2} \cdot \text{s}^{-1}$  at front side; obviously the back side takes more damage.

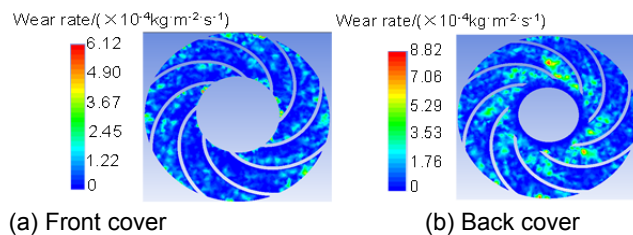


Figure 3: The wear distribution on impeller cover plate

Figure 4 shows wear distribution of impeller blades. It can be seen from Figure 4 that the suction surface of impeller blade suffers a wide range of wear; inlet of the blade is heavily eroded while the wear rate of middle part is lower and the outlet is barely intact. Erosive wear is mostly taken place at the bottom and the top in the pressure surface; the results are in agreement with Xu H. The suction surface (average wear rate  $1.46 \times 10^{-4} \text{ kg} \cdot \text{m}^{-2} \cdot \text{s}^{-1}$ ) takes more damage than the pressure surface (average wear rate  $4.36 \times 10^{-5} \text{ kg} \cdot \text{m}^{-2} \cdot \text{s}^{-1}$ ), and a larger wear area.

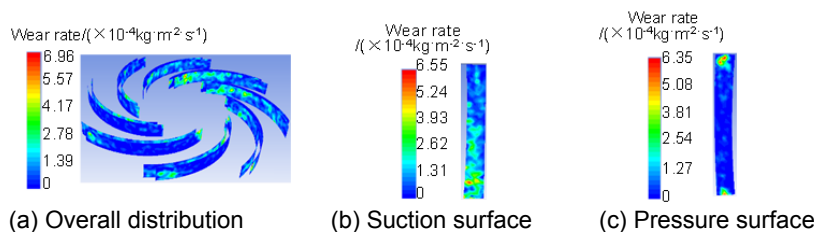


Figure 4: Wear distribution of impeller blades

(2) Guide impeller

Figure 5 is the wear distribution of impeller blades. It can be seen from Figure 5 that the area suffers from highest wear rate is in the central of inner surface, where the sealing ring placed, showcasing a circumferential distribution. Some individual points are particularly seriously eroded, becoming the most seriously eroded part of the pump (Figure 1a). Calculation results are consistent with the wear patterns. At the outlet of impeller blade, sand comes out at a high speed with liquid flow, causing the direct impact on the inner wall of the guide impeller where the wear rate is much higher than other places. Concave side erodes more seriously than convex side in guide impeller. In the concave side wear always happen at the outlet and inlet, central position shares an even distribution of wear, while wear place in convex side is located at the inlet of blade.

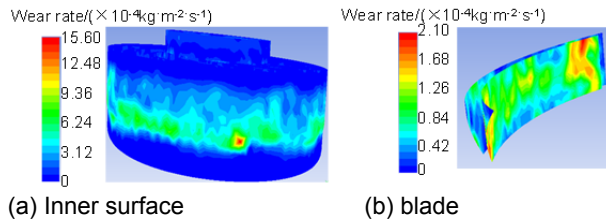


Figure 5: The wear distribution of impeller blades

#### 4. Effect on wear of ESP impellers by working condition and structural parameters

##### 4.1 Working condition parameters

The impeller is an essential component of centrifugal pump, providing energy for lifting the drilling fluid. Thus become the most vulnerable part of wear. Wear on the impeller wall will lead to a drop of efficiency by losing the original type line and series of consequences by imbalance of rotor. The influence on wear of ESP by different factors such as working conditions (sand grain size, sand concentration, pump speed) and impeller structural parameters (inlet and outlet angle) is discussed.

##### (1) Particle size and concentration rate

In practical environment, sand rate is required to be no more than 0.05%, however, it would be higher at initial stage of production. Therefore the simulation working condition is as follows, rated displacement: 50m<sup>3</sup>/d, solid phase volume fraction of solid phase: 0.03%, 0.05%, 0.1%, particle diameter: 0.03mm, 0.04mm, 0.05mm, 0.06mm, 0.07mm, 0.08mm.

At the sand concentration rate of 0.03%, 0.05%, and 0.1%, Change the particle size to calculate the influence on erosive wear by sand concentration rate and particle size. 0.03% is selected to analyse the erosive impact by particle size. Figure 6 is the wear cloud map at the sand concentration rate of 0.03%. It can be seen from Figure 6 that with the increase of the particle size, eroded area of impeller blade's suction surface becomes larger, the max wear rate first rise then decline. Pressure surface suffers a severe wear from bottom and top, with the increase of particle size, outlet takes more damage.

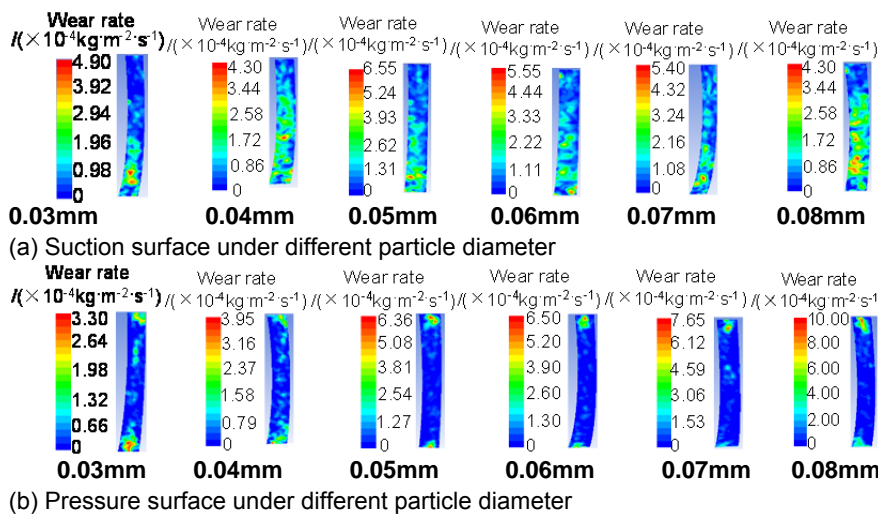


Figure 6: Wear cloud map at concentration rate of 0.03% under different particle sizes

Figure 7 shows the wear rate varying with particle size at different sand concentration rate. It can be seen from Figure 7 that higher concentration rate means higher wear rate. When concentration rate is set, wear rate will go up then go down with the increase of the particle size. Wear rate peaked at different particle size in different concentration rate, 0.05mm at 0.03%, 0.06mm at 0.05%, 0.06mm at 0.1%. At certain concentration rate, mass of the individual particles will increase with the increase of particle size but the number of particles will decrease, thereby reducing the number of collisions with the wall of the impeller, the average wear rate of impeller blade will increase at first then go down under the combined influence of the quantity and mass of the particles. When particle size is set, wear rate will go up with increase of concentration rate.

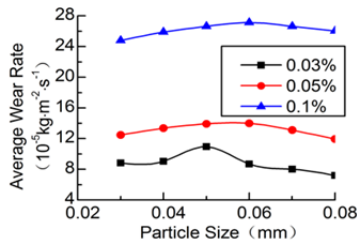


Figure 7: Average wear rate under different particle size and concentration rate

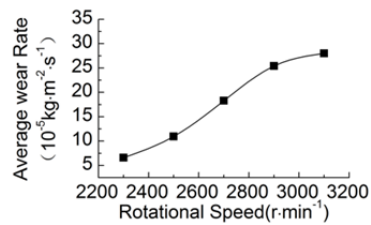


Figure 8: Average wear rate varies under different rotational speed

(2) Pump speed

Select pump speed at 2300r/min, 2500r/min, 2700r/min, 2900r/min and 3100r/min, solid phase volume fraction at 0.05%, particle diameter in 0.05 mm to analyse the effect by pump speed. Figure 8 is the average wear rate of different pump speed. According to Figure 8, higher pump speed causes more wear. If moderately reduce the rotor speed in the premise of meeting the basic working requirement, it will reduce the damage of the wear to a certain extent.

4.2 Structural parameters

(1) Inlet angle

Select the outlet angle  $\beta_2$  at 22°,  $\beta_1$  at 26°, 30°, 34°, 38°, 42°, solid phase volume fraction at 0.03%, particle size in 0.05mm, Figure 9 shows the results of average wear rate in different inlet angle.

It can be seen from Figure 9 that at a certain blade outlet angle ( $\beta_2=22^\circ$ ), with increase of inlet angle, wear rate of front cover faces a continuous downtrend, but decrease rate becomes lower. The wear rate of back cover faces a linear decline. Wear rate of front cover is higher than back cover when  $\beta_1 < 32^\circ$ , but after that the back cover outnumbered. With the increase of inlet angle, wear rate of suction surface shows a trend of fluctuation, peaked at 36° then faced a dramatic decline and reached its minimum value at 42°. Average wear rate of pressure surface was on a slight decline and always lower than the suction surface. The overall wear rate of impeller decreased with the rising of inlet angle. As a result, when the outlet angle is set ( $\beta_2=22^\circ$ ), with the increase of inlet angle, the average wear rate will decrease in general, thus a bigger inlet angle should be selected in design stage.

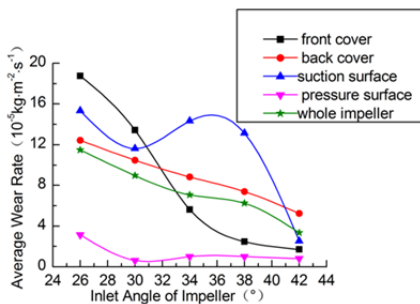


Figure 9: The average wear rate under different inlet angle

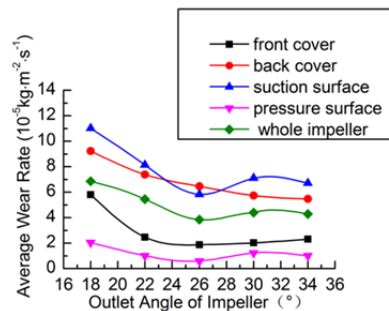


Figure 10: The average wear rate under different outlet angle

(2) Outlet angle

Select the inlet angle  $\beta_1$  at 38°,  $\beta_2$  at 18°, 22°, 26°, 30°, 34°, solid phase volume fraction at 0.03%, particle size in 0.05mm, Figure 10 shows the results of average wear rate in different outlet angle. It can be seen from

Figure 10 that at a certain blade inlet angle ( $\beta_1=38^\circ$ ), with increase of outlet angle, wear rate of front cover decrease first then slightly increase. The wear rate in back cover faces a continuous down trend but always higher than the front cover. The average wear rate of suction surface shows a trend of fluctuation (decrease first, increase and then decrease again), while the wear rate of pressure surface increase first then decrease, both of which reach their bottom at  $\beta_2=26^\circ$ . The average wear rate of impeller also reaches the lowest point at  $\beta_2=26^\circ$ . Therefore outlet angle of impeller should be neither too high nor too low.

## 5. Conclusion

- 1) Sever erosive wear are located at head and middle part of suction surface, as well as the inlet and outlet of pressure surface. Inner wall of guide impeller that corresponding to impeller outlet are the most eroded area. Thus protective coating in those areas will help to reduce the erosive wear.
- 2) With the increase of sand concentration rate and pump speed, wear rate will rise. When the concentration rate is set, wear rate will first go up then go down with the rising of particle size.
- 3) The average wear rate will go down with increase of inlet angle, while the increase of outlet angle will make it increase and then decrease. Therefore in design stage, it is better to select a higher inlet angle, while the outlet angle should be neither too high nor too low.

## Acknowledgment

This work was financially supported by Natural fund of Shandong Province (Approval No. ZR2015EL012).

## References

- Chen S., Wang Z., Lv F., He J., 2015, Numerical calculation of particle erosion within electric submersible pump based on discrete phase model, *Journal of China University of Petroleum*, 39, 3, 143-148, DOI: 10.3969/j.issn.1673-5005.2015.03.020.
- Khalid Y.A., Sapuan S.M., 2007, Wear analysis of centrifugal slurry pump impellers, *Industrial Lubrication and Tribology*, 55, 18-28, DOI: 10.1108/00368790710723106.
- Lee S.Y., Dimenna R.A., Duignan M.R., 2002, Designing a scaled erosion test with computational fluid dynamics methods, *ASME 2002 Joint U.S.-European Fluids Engineering Division Conference*, 2, 223-230, DOI: 10.1115/FEDSM2002-31285.
- Pagalthivarthi K.V., Desai P.V., Addie G.R., 2007, Particulate motion and concentration fields in centrifugal slurry pumps, *Particulate Science and Technology*, 24, 77-96, DOI: 10.1080/02726359008906557.
- Pagalthivarthi K.V., Gupta P.K., Tyagi V., Ravi M.R., 2011, CFD predictions of dense slurry flow in centrifugal pump casings, *World Academy of Science, Engineering and Technology*, 5, 538-550, DOI: scholar.waset.org/1999.8/3699.
- Roudnev A, Bourgeois R.J., Kosmicki R.J., 2009, Slurry pump casing wear prediction using numerical multi-phase flow simulation, *ASME 2009 Fluids Engineering Division Summer Meeting*, 1, 515-523, DOI: 10.1115/FEDSM2009-78564.
- Wang Z., Mei S., Chen S., Lv F., Yan L., 2014, Numerical simulation and verification of particle impact erosion within electric submersible pump, *Journal of Southwest Petroleum University*, 4, 175-181, DOI: 10.11885/j.issn.1674-5086.2014.01.23.03.